2012

Donor behavior of Sb in ZnO

H. Y. Liu
Virginia Commonwealth University

N. Izyumskaya
Virginia Commonwealth University, nizioumskaia@vcu.edu

Vitaliy Avrutin
Virginia Commonwealth University, vavrutin@vcu.edu

See next page for additional authors

Liu, H. Y., Izyumskaya, N., & Avrutin V., et al. Donor behavior of Sb in ZnO. Journal of Applied Physics, 112, 033706 (2012).

Donor behavior of Sb in ZnO

H. Y. Liu,[1] N. Izyumskaya,[1] V. Avrutin,[1] Ü. Özgür,[1] A. B. Yankovich,[2] A. V. Kvit,[2] P. M. Voyles,[2] and H. Morkoç[1,a)]
[1]*Department of Electrical and Computer Engineering, Virginia Commonwealth University, Richmond, Virginia 23284, USA*
[2]*Department of Materials Science & Engineering, University Wisconsin-Madison, Madison, Wisconsin 53706, USA*

(Received 13 May 2012; accepted 5 July 2012; published online 3 August 2012)

Electrical behavior of Sb in ZnO:Sb layers doped in a wide concentration range was studied using temperature dependent Hall effect measurements. The layers were grown by plasma-enhanced molecular beam epitaxy, and the Sb concentration was changed by varying the Sb flux, resulting in electron concentrations in the range of 10^{16} to nearly $10^{20}\,cm^{-3}$. Upon annealing, the electron concentration increased slightly and more notable was that the electron mobility significantly improved, reaching a room-temperature value of 110 $cm^2/V\,s$ and a low-temperature value of 145 $cm^2/V\,s$, close to the maximum of ~155 $cm^2/V\,s$ set by ionized impurity scattering. Hall data and structural data suggest that Sb predominantly occupies Zn sublattice positions and acts as a shallow donor in the whole concentration range studied. In the layers with high Sb content (~1 at. %), acceptor-type compensating defects (possibly Sb on oxygen sites and/or point-defect complexes involving Sb_O) are formed. The increase of electron concentration with increasing oxygen pressure and the increase in ZnO:Sb lattice parameter at high Sb concentrations suggest that acceptors involving Sb_O rather than Sb_{Zn}-$2V_{Zn}$ complexes are responsible for the compensation of the donors. © *2012 American Institute of Physics*. [http://dx.doi.org/10.1063/1.4742984]

I. INTRODUCTION

Owing to a wide band gap of ~3.3 eV at room temperature and a large exciton binding energy of 60 meV, ZnO holds great promise for various applications in electronic and optoelectronic devices.[1,2] The absence of reliable *p*-type doping is the major bottleneck limiting the development of various types of bipolar ZnO-based devices,[1,3] including light-emitting and laser diodes. The *p*-type problem has been ascribed to self-compensation of acceptors by native donor defects (V_O and Zn_i),[4] incorporation of hydrogen donors from the growth environment,[5] low acceptor dopant solubility limits, and deep acceptor levels.[6] In an effort to establish reliable *p*-type doping of ZnO, a great deal of attention has been focused on the *group VA* elements N, P, As, and Sb, which would be expected to generate acceptor states if incorporated substitutionally on the oxygen sites. It should be noted that the ionic radii of all the aforementioned elements are larger than that of oxygen. Therefore, nitrogen, with the smallest ionic radius among the *group VA* elements, is thought of the best candidate for *p*-type doping in ZnO. However, *p*-type doping with nitrogen (including co-doping[7]) has resulted only in limited success in terms of stability and hole mobility. Nitrogen creates a relatively deep acceptor level of 0.165 eV,[8,9] has a low solubility limit, and has the tendency to self-compensate via the formation of donor-type complexes, such as N_2 on O sites and Zn_i-N_O.[10–12]

Other *group V* elements, including P,[6,13–16] As,[17–20] and Sb[21–23] have also been reported to lead to *p*-type ZnO. However, reproducibility of the results and stability of the *p*-type conductivity are under question. For example, the *p*-type conductivity of ZnO:Sb reported by Aoki *et al.*[22] might come under question because the reported hole concentration of $5 \times 10^{20}\,cm^{-3}$ is extremely high. Similarly, it is fair to state that questions might also arise regarding the light-emitting diodes based on *p*-ZnO:Sb/*n*-ZnO:Ga homojunctions[24] which exhibit extremely low light output power, inconsistent with the earlier reported hole concentrations and mobilities.[23] Fundamentally, since the ionic radii of the *group V* elements, especially As^{3-} (2.11 Å) and Sb^{3-} (2.44 Å), far exceed that of O^{2-} (1.38 Å),[25,26] they are more likely to occupy Zn sites (ionic radii are 0.58 Å for As^{3+} and 0.76 Å for Sb^{3+} vs. 0.6 Å for Zn^{2+})[26] and act as donors. Indeed, using the emission channeling technique, Wahl *et al.* found that the majority of implanted As (Ref. 17) and Sb (Ref. 27) ions occupy Zn sites in ZnO.

In an attempt to explain the acceptor behavior of the large *group V* elements (As, Sb) in ZnO, Limpijumnong *et al.*[28] proposed a model based on first-principle calculations. In this model, the large-size-mismatched *group V* dopant ions occupy Zn sites but form a complex with two spontaneously induced Zn vacancies. These As_{Zn}–$2V_{Zn}$ or Sb_{Zn}–$2V_{Zn}$ complexes create shallow acceptor levels and are responsible for *p*-type conductivity. However, Janotti and Van de Walle[29] have pointed out that the formation of these complexes is unlikely from an energetic point of view, and entropic considerations argue against their formation because the complexes are comprised three constituents. Puchala and Morgan[30] have recently showed that there is a more stable configuration in which the As or Sb atom occupies an interstitial position, leaving behind another Zn vacancy, so the

a)E-mail: hmorkoc@vcu.edu. Telephone: +1 804 827 3765. Fax: +1 804 827 0006.

entire complex is $(As,Sb)_I$-$3V_{Zn}$. This complex generates a deep level, so it is not effective acceptor. It should be also noted that four constituents involved into this complex make the probability of its formation very low.

In this work, we undertook an experimental investigation of the conduction type and carrier concentration and mobility in ZnO doped with Sb in a wide range of concentrations using temperature dependent Hall effect measurements and correlated these data with structural data. The ZnO:Sb layers have been grown by radio-frequency plasma-enhanced molecular beam epitaxy (PE-MBE), and Sb concentration was tailored by varying the Sb flux, resulting in a variation in electron carrier concentration from 10^{16} to nearly $10^{20}\,cm^{-3}$. A consistent explanation of all the data is that Sb predominantly occupies Zn positions and acts as shallow donors in the whole concentration range studied.

II. EXPERIMENTAL

Sb-doped ZnO (ZnO:Sb) layers ~200 nm thick were grown on *a*-plane sapphire substrates by plasma enhanced MBE. For enhanced nucleation, 5-nm-thick low-temperature (300 °C) ZnO buffer layers were inserted between the substrates and the ZnO:Sb films. The growth of the ZnO:Sb films was monitored by *in situ* reflection high energy electron diffraction (RHEED). The Zn cell temperature was fixed at 350 °C for all samples. Three sets of samples were studied.

First, to investigate the effect of Sb doping, a series of samples with different Sb content were grown. The concentration of Sb in the layers was controlled by varying the Sb flux via changing the Sb cell temperature, T_{Sb}, from 370 °C to 570 °C. The substrate temperature was kept constant at 400 °C, and the oxygen pressure, P_{O_2}, during growth was set at 9×10^{-6} Torr to provide near-stoichiometric growth conditions[31] (reactive oxygen-to-metal flux ratio of ~1).

Second, to study the effect of substrate temperature, we grew a set of four samples at a substrate temperature of 400 °C or 600 °C with $T_{Sb} = 400$ and 550 °C.

Third, to study the effect of P_{O_2} on electrical properties of ZnO:Sb, we grew a series of layers at $P_{O_2} = 4.5 \times 10^{-6}$ Torr (metal-rich conditions, reactive oxygen-to-metal flux ratio < 1), 9×10^{-6} Torr (near-stoichiometric conditions), and 1.5×10^{-5} Torr (oxygen-rich conditions, reactive oxygen-to-metal flux ratio > 1), with fixed T_{Sb} and substrate temperature.

To study the effect of thermal treatment, post-growth rapid thermal annealing (RTA) at ~600 °C in nitrogen environment for 3 min was employed for selected ZnO:Sb samples.

To rule out the possibility that the electrical properties of ZnO:Sb films are affected by Al out-diffusion from the sapphire substrate, several samples were duplicated on 330-μm-thick bulk ZnO substrates (CrysTec GmbH). To produce a surface with atomic steps, the ZnO substrates were annealed in air at 1050 °C prior to loading into the MBE system. Approximately 300-nm thick ZnO:Sb and undoped ZnO layers were grown at $P_{O_2} = 9 \times 10^{-6}$ Torr with different T_{Sb} of 0, 430, and 525 °C.

The crystal structure of the layers was characterized by high-resolution x-ray diffraction (HRXRD) and scanning transmission electron microscopy (STEM). STEM images were acquired with a 24.5 mrad semi angle probe, 24.5 pA probe current, and ~0.8 Å resolution. Low angle annular dark field (LAADF) STEM images with a STEM detector range of 28.8 to 143.8 mrad were used to emphasize strain contrast from defects.

Carrier concentration and mobility in the ZnO:Sb layers were obtained from the Hall measurements in the van der Pauw configuration at room temperature for all samples. For selected samples, Hall measurements were performed as a function of temperature.

III. RESULTS

The Hall effect measurements at room temperature revealed *n*-type conductivity in all the ZnO:Sb layers grown in a wide range Sb fluxes and thus in a wide range of Sb concentrations. Figure 1(a) shows the electron concentration as a function of Sb cell temperature, T_{Sb}. Note that the electron concentration first rises exponentially with T_{Sb}, then saturates at about $7.6 \times 10^{19}\,cm^{-3}$ (region 1 in Fig. 1), and finally drops to $1 \times 10^{17}\,cm^{-3}$ as T_{Sb} is further increased from 480 to 550 °C (region 2 in Fig. 1). A further increase in T_{Sb} up to 570 °C (not shown) produces insulating ZnO:Sb films with resistance ranging from tens to hundreds of MΩ, preventing reliable Hall measurements, indicative of highly compensated material.

The increase in electron concentration with T_{Sb} in region 1 is due to increasing Sb concentration in the films. For samples grown at $T_{Sb} = 430$ °C (region 1) and $T_{Sb} = 520$ °C (region 2), the Sb content was measured by STEM energy dispersive spectroscopy (EDS) on cross-section samples. The Sb concentration was found to be below the EDS detection limit (estimated at ~0.1 at. %) for the first sample, and 0.9 at. % for the second. The initial increase in electron

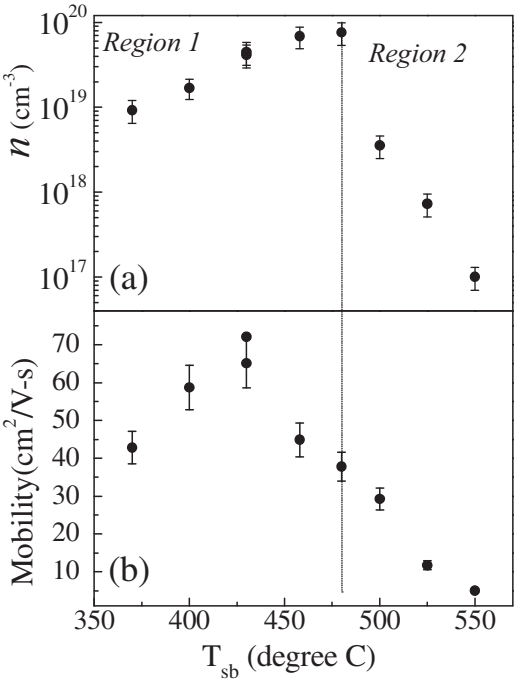

FIG. 1. (a) Electron concentration and (b) mobility in as-grown ZnO:Sb layers as functions of T_{Sb}.

concentration indicates that the increasing Sb concentration creates donors. The decrease in electron concentration with further increasing T_{Sb} in region 2 may be explained by formation of Sb-containing acceptor-type compensating defects, as discussed below.

The properties of ZnO:Sb on bulk ZnO substrates were similar to those of ZnO:Sb on sapphire. We measured three layers on bulk ZnO substrates; one that was nominally undoped, the second grown with $T_{Sb} = 430\,^{\circ}\mathrm{C}$ (region 1), and the third grown with $T_{Sb} = 525\,^{\circ}\mathrm{C}$ (region 2). Similar to their counterparts on sapphire, the nominally undoped ZnO film and the heavily doped film grown with $T_{Sb} = 525\,^{\circ}\mathrm{C}$ were highly resistive (20–30 kΩ for probe separation of 2–3 mm). Because the layers were grown on conductive ZnO substrates, we were not able to derive reliable values of carrier concentration, as parallel conduction through the ZnO substrate becomes a complicating factor.

The layer grown with $T_{Sb} = 430\,^{\circ}\mathrm{C}$ was conductive with a resistance of 200–300 Ω measured with 2 probes on the layer separated by 2–3 mm, which is comparable to its counterpart grown on sapphire. Hall effect measurements performed with contacts formed on the film side of this sample yielded a Hall mobility of ~90 $\mathrm{cm^2/V\,s}$ and a sheet electron density of $4.11 \times 10^{14}\,\mathrm{cm^{-2}}$. Because the ZnO substrate is also conductive, its contribution to the electrical properties of the sample must be assessed. Although the electron concentration in the ZnO substrate is relatively low (10^{14} to $10^{15}\,\mathrm{cm^{-3}}$ range), its contribution to the Hall measurements may be substantial because of the relatively large substrate thickness (330 μm). The electrical properties of hydrothermal ZnO substrates heat-treated in air and then in vacuum during the MBE growth can differ from those of as-received ones. For this reason, we performed Hall effect measurements with contacts applied on the back side of the substrate for the undoped, non-conducting ZnO layer. The total mobility and sheet carrier density for the ZnO substrate were ~80 $\mathrm{cm^2/V\,s}$ and $4.93 \times 10^{13}\,\mathrm{cm^{-2}}$, respectively. Using the double-layer analysis[32,33] in which the first conducting layer is taken as the ZnO:Sb film and the second one as bulk ZnO, we calculated the electron concentration in the ZnO:Sb thin film grown with $T_{Sb} = 430\,^{\circ}\mathrm{C}$ to be $\sim 1.3 \times 10^{19}\,\mathrm{cm^{-3}}$, which is close to the value obtained for its counterpart grown on sapphire ($4.4 \times 10^{19}\,\mathrm{cm^{-3}}$). The minor difference in the carrier density may be due to (1) out-diffusion of alkali metals (Li and Na) from the bulk ZnO substrate fabricated by hydrothermal growth technique, which act as compensating acceptors; (2) the inaccuracy introduced by the double-layers analysis, and (3) the possible Al out-diffusion from sapphire substrate supplying additional donors to the ZnO:Sb layers.

Figure 1(b) shows the Hall mobility in ZnO:Sb layers grown on sapphire as a function of T_{Sb}. In region 1, the Hall mobility first rises from 43 cm to ~70 $\mathrm{cm^2/V\,s}$ as T_{Sb} increases from 370 °C to 430 °C, and then drops down to 5 $\mathrm{cm^2/V\,s}$ with the further increase of T_{Sb} from 430 °C to 550 °C. Figure 2 shows temperature-dependent Hall effect data on the samples grown with $T_{Sb} = 460\,^{\circ}\mathrm{C}$ (the second highest electron concentration), $T_{Sb} = 430\,^{\circ}\mathrm{C}$ (the highest mobility) and the annealed sample with the highest mobility. The carrier concentration in all the samples is temperature independent, indicating that they are degenerate. The

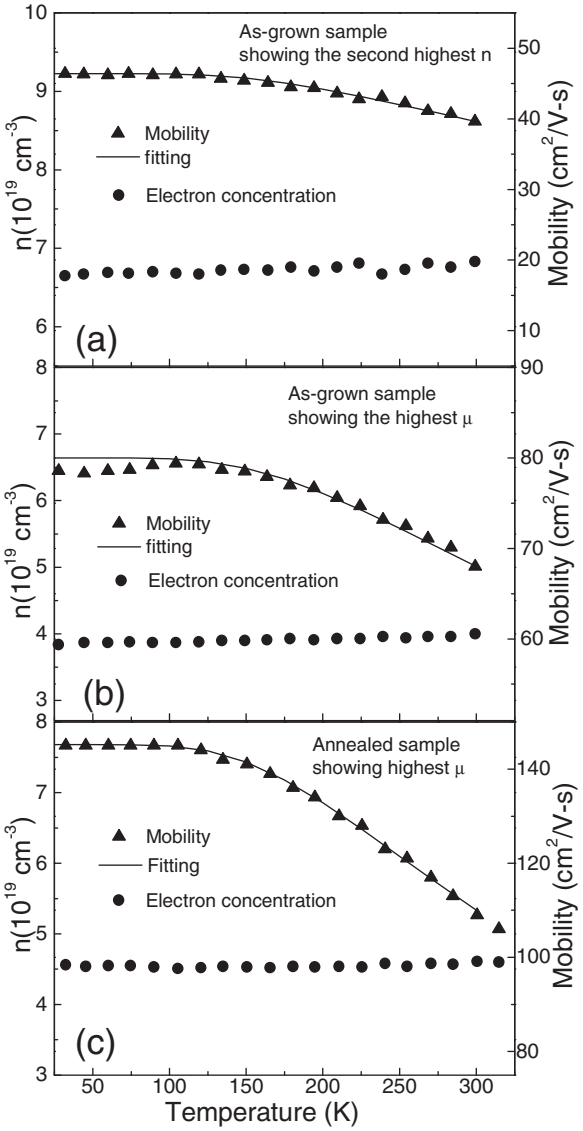

FIG. 2. Temperature dependence of the electron concentration and mobility for as-grown ZnO:Sb samples with (a) the second highest electron concentration and (b) the highest mobility and (c) for the annealed sample with the highest mobility. Solid curves are the result of fitting by the method described in Ref. 35.

temperature dependence of mobility can shed light on the dominant carrier scattering mechanism. In heavily doped ZnO (carrier concentrations $> 10^{19}\,\mathrm{cm^{-3}}$), three major mechanisms can contribute to the electron scattering: scattering on grain boundaries, scattering on ionized impurities, and scattering on polar optical phonons.[34,35] The former two mechanisms are operative in a wide temperature range, while the latter one becomes important at temperatures above 150 K in high-quality material with dominating ionized-impurity scattering. For all our samples, the mobility is independent of temperature below ~150 K, suggesting that ionized impurity scattering dominates.[35] The reduction in mobility above ~150 K is attributable to the contribution of polar-phonon scattering.[35] The temperature dependences of the mobility show no signature of grain boundary scattering.[35]

The increase in mobility with T_{Sb} in region 1 (Fig. 1(b)) can be explained by screening of ionized impurities by free

electrons whose concentration also rises with T_{Sb}. The decrease in the mobility with further increase in Sb content may be attributed to the formation of compensating defects in the layers grown with $T_{Sb} > 430\,^{\circ}\mathrm{C}$. Degradation of the structural quality of ZnO:Sb with increasing Sb content, evident from XRD and TEM data discussed below, may also play a role. Upon annealing, the electron concentration increases slightly and the electron mobility is significantly improved (Fig. 2(c)). The annealed sample shows a room-temperature mobility of 110 cm^2/V s and a low temperature mobility of 145 cm^2/V s, which is close to the maximum mobility ($\sim$155 cm^2/V s for donor concentration of $4.5 \times 10^{19}\,cm^{-3}$) calculated from the degenerate form of Brooks-Herring formula for ionized impurity scattering.[33]

Figure 3(a) shows the out-of-plane c lattice parameter derived from 2θ-ω HRXRD scans as a function of T_{Sb}. For T_{Sb} up to 500 °C (the entire region 1 and a portion of region 2 in Fig. 1(a)), the c lattice parameter varies only slightly around the bulk ZnO value of 5.206 Å. However, it abruptly increases to 5.296 Å for $T_{Sb} = 520\,^{\circ}\mathrm{C}$ and continues to increase for the layer grown with $T_{Sb} = 550\,^{\circ}\mathrm{C}$. Figure 3(b) shows the full width at half maximum (FWHM) of the (0002) XRD ω-rocking curves as a function of T_{Sb}. The FWHM remains virtually unchanged (FWHM $\sim 0.53^{\circ}$) with T_{Sb} in region 1, then increases rapidly in region 2 ($T_{Sb} \geq 480\,^{\circ}\mathrm{C}$). The broad XRD ω-rocking curves point to inferior crystal quality of ZnO with high Sb concentration. This finding is in agreement with the electrical data (Fig. 1) pointing to defect formation in heavily doped layers.

Figures 4(a) and 4(b) display cross-sectional STEM images of the sample with low Sb content grown with

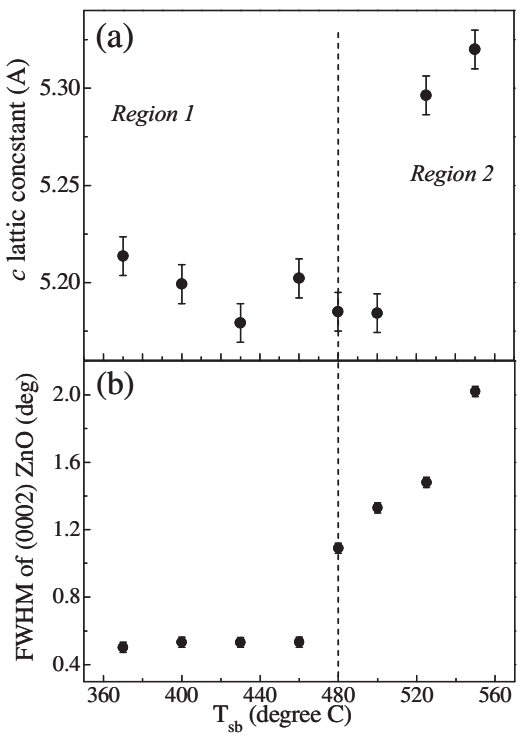

FIG. 3. (a) Out-of-plane c lattice parameter derived from 2θ-ω HRXRD scans and (b) FWHM of (0002) ZnO:Sb XRD ω-rocking curves as a function of T_{Sb}.

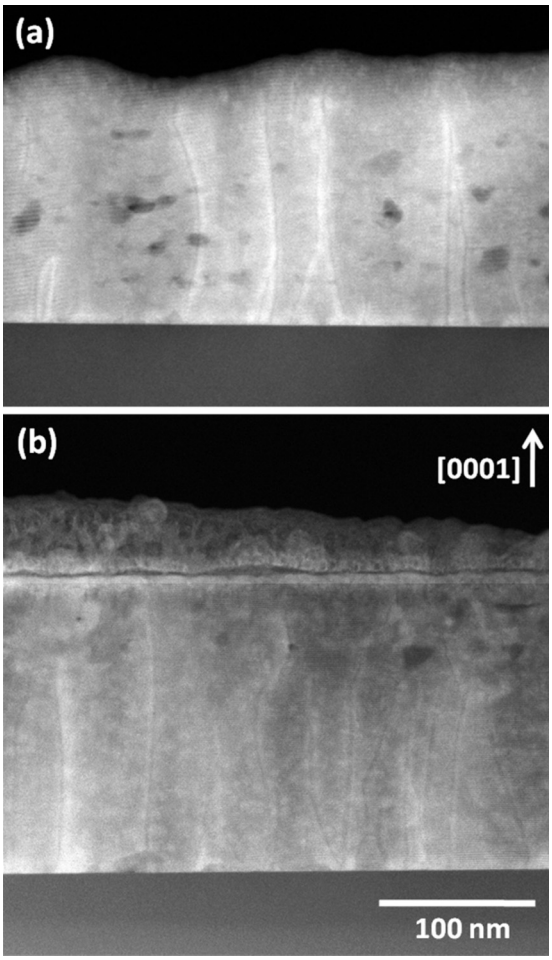

FIG. 4. Cross-sectional LAADF STEM images of samples with (a) low Sb content ($T_{Sb} = 430\,^{\circ}\mathrm{C}$) and (b) high Sb content ($T_{Sb} = 520\,^{\circ}\mathrm{C}$) showing that dislocations and voids are the dominant extended defect in both samples.

$T_{Sb} = 430\,^{\circ}\mathrm{C}$ and the sample with high Sb content grown with $T_{Sb} = 520\,^{\circ}\mathrm{C}$, respectively. As can be seen pores and dislocations are the predominant defects. We should state that appearance of pores is not a STEM sample preparation artifact and has also been observed in ZnO layers heavily doped with Ga.[35] The density of dislocations in the Sb doped ZnO layers is $4 \pm 1 \times 10^{10}$ dislocations/cm^2, estimated from the abovementioned images and STEM electron energy loss spectroscopy measurement of the local samples thickness.[36] Within the 25% uncertainty caused by the limited viewable area in cross-section STEM samples, there is no difference in dislocation density between samples grown with $T_{Sb} = 430\,^{\circ}\mathrm{C}$ and 520 °C.

Figures 5(a) and 5(b) show the effect of oxygen pressure P_{O_2} during growth on electron mobility and electron concentration in the ZnO:Sb layers with low Sb concentrations (region 1). For the layers grown under Zn-rich conditions ($P_{O_2} = 4.5 \times 10^{-6}$ Torr), both concentration and mobility are considerably lower than those for the samples grown at higher oxygen pressures.

Table I compares the electrical characteristics of films grown at $T_{Sb} = 400\,^{\circ}\mathrm{C}$ (region 1) and 550 °C (region 2) at substrate temperatures of 400 and 600 °C. One can see that the increased substrate temperature results in a decrease in electron concentration and mobility for both region 1 and region 2.

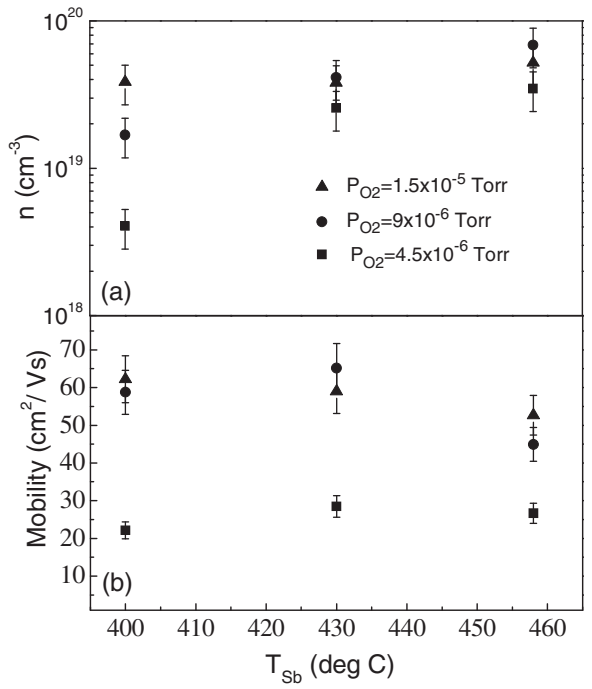

FIG. 5. Effect of oxygen pressure, P_{O_2}, on (a) electron concentration and (b) mobility for the ZnO:Sb layers grown with low Sb flux (region 1).

Since high P_{O_2} and post-growth oxygen annealing have been reported to enhance hole concentration or even switch *n*-type ZnO(As,Sb) to *p*-type,[28] possibly by creating Zn vacancies for (As,Sb)-2V_{Zn} clusters, we grew ZnO:Sb layers with different oxygen pressures, $P_{O_2} = 4.5 \times 10^{-6}$, 9×10^{-6}, and 1.5×10^{-5} Torr, and the remaining parameters were selected from our previous results for minimum electron concentration: high substrate temperature (600 °C) and high Sb flux ($T_{Sb} = 550$ °C, region 2). In all cases, the ZnO:Sb was still *n*-type. In the first and second cases, the electron concentrations are in the mid-10^{16} cm^{-3} range, while electron mobilities are ~2–3.7 cm^2/V s, resulting in a resistivity around 27–42 Ω cm. For the sample grown at $P_{O_2} = 1.5 \times 10^{-5}$ Torr, the resistivity varied around 400 Ω cm but the measured carrier concentration and mobility depend on the measurement conditions (applied magnetic field of 5–7 kG and current of 5–20 nA) and, consequently, are not reliable. The unreliability could result from strong localization of free carriers caused by high defect concentrations in the sample.

IV. DISCUSSION

All of our experimental data lead to the conclusion that Sb acts primarily as a donor, not an acceptor, in ZnO. This is true for all substrate temperatures, Sb concentrations, and P_{O_2}, in the as-deposited and annealed states, and on sapphire and bulk ZnO substrates. Similar results were found by Zhu *et al.*,[37] who reported electron concentrations ranging from 1.6 to 5.78×10^{19} cm^{-3} in ZnO:Sb layers grown on glass substrates by pulsed laser deposition.

TABLE I. Effect of substrate temperature effects on electrical properties of ZnO:Sb films.

T_{sb}, °C	T_{substr}, °C	n, cm^{-3}	μ, cm^2/V s	ρ, Ω cm
(Region 1)	400	1.68×10^{19}	58.73	0.0063
400	600	1.39×10^{19}	39.27	0.0117
(Region 2)	400	10×10^{16}	5.03	12.5
550	600	6.7×10^{16}	2.17	42.6

We propose that, at low Sb concentrations, Sb species incorporate on the Zn sites and act as donors, and at high Sb concentrations, some Sb atoms begin to incorporate on the O sites or form point defect complexes that act as acceptors; however, they are unlikely to be Sb_{Zn}–2V_{Zn}, since an abrupt increase in the lattice parameter (shown in Fig. 3(b)) cannot be expected in this case. This hypothesis is consistent with all of our electrical and structural data. In Fig. 1, the initial increase in the electron concentration in region 1 is explained by increasing donor Sb incorporation on Zn sites. In this region, the *c* lattice parameter shown in Fig. 3(a) is essentially unchanged, because the ionic radius of Sb^{3+} (0.76 Å) is close to that of Zn^{2+} (0.6 Å). In region 2, the decrease in electron concentration with further increases in T_{Sb} is explained by the formation of Sb-containing compensating acceptor defects, such as Sb_O. The large jump in *c* lattice parameter occurs due to a change in site occupation for some of the Sb ions, potentially in the O sublattice, since the ionic radius of Sb^{3-} (2.44 Å) far exceeds that of O^{2-} (1.38 Å).

An increase in dislocation density with increasing Sb content in ZnO:Sb has been reported by Guo *et al.*[3] Although no increase was seen in our STEM data, higher dislocation density may be the cause of considerable broadening of the XRD rocking curves in region 2 of Fig. 3(b). We suggest that this may be explained by large lattice distortions arising from Sb incorporation on the O sites, paving the way for dislocation formation.

The effect of P_{O_2} (Fig. 5) is also consistent with the formation of Sb_{Zn} donors. Zn-rich conditions (low P_{O_2}) suppress incorporation of Sb on Zn sites and formation of Sb_{Zn} donors, resulting in low electron concentration. On the other hand, high P_{O_2} (Zn-deficient conditions) favors incorporation of Sb on Zn sites and suppresses the incorporation of Sb on O sites. Both factors lead to higher electron concentration and mobility. Figure 5 shows the saturation in electron concentration as T_{Sb} approaches 480 °C, independent of P_{O_2}, which is also the boundary between region 1 and region 2 in Fig. 1. This behavior suggests a solubility limit for Sb ions on the Zn sites. Above this Sb concentration limit, we propose that some Sb species begin to incorporate into the oxygen sites, which is consistent with the XRD data showing a rapid degradation of ZnO:Sb crystallinity with increasing T_{Sb} in region 2, as illustrated in Fig. 3(b). Sb may be involved in Sb-containing point-defect complexes, some of which can act as acceptors, but the P_{O_2} data in Fig. 5 are inconsistent with acceptor Sb_{Zn}-2V_{Zn} complexes. The concentration of Sb_{Zn}-2V_{Zn} complexes should increase with P_{O_2}, since the probability of Zn vacancy formation is higher for high P_{O_2}. As a result, the compensation ratio should increase, and the electron concentration should decrease with increasing P_{O_2}, which is not the case as seen in Fig. 5. Therefore, one can conclude that Sb_O acceptors rather than Sb_{Zn}-2V_{Zn}

complexes are responsible for the compensation of Sb_{Zn} donors. Finally, the reduced electron concentration and mobility observed at higher substrate temperatures shown in Table I could be explained by the relatively lower incorporation efficiency of Sb on Zn sites and the formation of acceptor-type defects compensating donors.

V. CONCLUSION

We studied the electrical behavior of MBE-grown ZnO:Sb layers, wherein Sb concentration was controlled by varying the Sb flux. Sb was found to act as a donor in a wide range of concentration producing electron densities ranging from 10^{16} to nearly $10^{20}\,cm^{-3}$. Upon annealing, the electron concentration increased slightly and the electron mobility significantly improved, reaching a room-temperature value of 110 cm^2/V s and a low-temperature value of 145 cm^2/V s along with an electron concentration of $\sim 4.5 \times 10^{19}\,cm^{-3}$ for a layer with a low Sb content of ~0.1 at. %. Based on Hall effect measurements XRD data, we conclude that Sb predominantly occupies Zn positions and acts as a donor in the whole concentration range studied. At high Sb content (~1 at. %), acceptor-type compensating defects, most likely Sb on oxygen sites, are formed, leading to a decrease in net electron concentration. The increase of electron concentration with increasing oxygen pressure at relatively low Sb concentrations (~0.1 at. %) and the increase in ZnO:Sb lattice parameter at high Sb concentrations (~1 at. %) both suggest that Sb_O acceptors rather than Sb_{Zn}-$2V_{Zn}$ complexes are responsible for the compensation of the donors.

ACKNOWLEDGMENTS

We acknowledge funding from the Department of Energy, Basic Energy Sciences (DE-FG02-08ER46547) and the Air Force Office of Scientific Research (FA9550-09-0447).

[1]V. Avrutin, D. Silversmith, and H. Morkoç, Proc. IEEE **98**, 1269 (2010).
[2]Ü. Özgür, Y. I. Alivov, C. Liu, A. Teke, M. A. Reshchikov, S. Doğan, V. Avrutin, S.-J. Cho, and H. Morkoç, J. Appl. Phys. **98**, 041301 (2005).
[3]W. Guo, A. Allenic, Y. B. Chen, X. Q. Pan, Y. Che, Z. D. Hu, and B. Liu, Appl. Phys. Lett. **90**, 242108 (2007).
[4]S. B. Zhang, S. H. Wei, and A. Zunger, Phys. Rev. B **63**, 075205 (2001).
[5]C. G. Van de Walle, Phys. Rev. Lett. **85**, 1012 (2000).
[6]C. H. Park, S. B. Zhang, and S.-H. Wei, Phys. Rev. B **66**, 073202 (2002).
[7]K. Nakahara, H. Takasu, P. Fons, A. Yamada, K. Iwata, K. Matsubara, R. Hunger, and S. Niki, Appl. Phys. Lett. **79**, 4139 (2001).
[8]F. Reuss, C. Kirchner, T. Gruber, R. Kling, S. Maschek, W. Limmer, A. Waag, and P. Ziemann, J. Appl. Phys. **95**, 3385 (2004).
[9]B. K. Meyer, J. Sann, D. M. Hofmann, C. Neumann, and A. Zeuner, Semicond. Sci. Technol. **20**, S62 (2005).
[10]F. Friedrich, M. A. Gluba, and N. H. Nickel, Appl. Phys. Lett. **95**, 141903 (2009).
[11]C. L. Perkins, S. H. Lee, X. N. Li, S. E. Asher, and T. J. Coutts, J. Appl. Phys. **97**, 034907 (2005).
[12]S. Limpijumnong, X. Li, S.-H. Wei, and S. B. Zhang, Appl. Phys. Lett. **86**, 211910 (2005).
[13]Y. W. Heo, Y. W. Kwon, Y. Li, S. J. Pearton, and D. P. Norton, Appl. Phys. Lett. **83**, 1128 (2003).
[14]F. G. Chen, Z. Ye, W. Xu, B. Zhao, L. Zhu, and J. Lv, J. Cryst. Growth **281**, 458 (2005).
[15]V. Vaithianathan, K. Asokan, J. Y. Park, and S. S. Kim, Appl. Phys. A: Mater. Sci. Process. **94**, 995 (2009).
[16]M. S. Oh, D. K. Hwang, Y. S. Choi, J. W. Kang, S. J. Park, C. S. Hwang, and K. I. Cho, Appl. Phys. Lett. **93**, 111905 (2008).
[17]U. Wahl, E. Rita, J. G. Correia, A. C. Marques, E. Alves, J. C. Soares, and ISOLDE Collaboration, Phys. Rev. Lett. **95**, 215503 (2005).
[18]M. Kumar and S. Y. Choi, Appl. Surf. Sci. **255**, 2173 (2008).
[19]V. Vaithianathan, B. T. Lee, C. H. Chang, K. Asokan, and S. S. Kim, Appl. Phys. Lett. **88**, 112103 (2006).
[20]V. Vaithianathan, S. S. Kim, and K. Asokan, Appl. Phys. Lett. **92**, 236101 (2008).
[21]T. Aoki, Y. Hatanaka, and D. C. Look, Appl. Phys. Lett. **76**, 3257 (2000).
[22]T. Aoki, Y. Shimizu, A. Miyake, A. Nakamura, Y. Nakanishi, and Y. Hatanaka, Phys. Status Solidi B **229**, 911 (2002).
[23]L. J. Mandalapu, Z. Yang, F. X. Xiu, D. T. Zhao, and J. L. Liu, Appl. Phys. Lett. **88**, 092103 (2006).
[24]S. Chu, J. Z. Zhao, Z. Zuo, J. Y. Kong, L. Li, and J. L. Liu, J. Appl. Phys. **109**, 123110 (2011).
[25]G. Bergerhoff, B. Kilger, C. Witthauer, R. Hundt, and R. Sievers, See http://cci.lbl.gov/cctbx_sources/cctbx/eltbx/icsd_radii.cpp for "Inorganic Crystal Structure Database in conjunction with Crystal Structure Information System and its application to CCDF—Cambridge Crystallographic Data File and MDF—Metal Data File," Bonn, 1986.
[26]R. D. Shannon, Acta Crystallogr., Sect. A: Cryst. Phys., Diffr., Theor. Gen. Crystallogr. **32**, 751 (1976).
[27]U. Wahl, J. G. Correia, T. Mendonca, and S. Decoster, Appl. Phys. Lett. **94**, 261901 (2009).
[28]S. Limpijumnong, S. B. Zhang, S. H. Wei, and C. H. Park, Phys. Rev. Lett. **92**, 155504 (2004).
[29]A. Janotti and C. G. Van de Walle, Rep. Prog. Phys. **72**, 126501 (2009).
[30]B. Puchala and D. M. Morgan, Phys. Rev. B **85**, 195207 (2012).
[31]H. Y. Liu, V. Avrutin, N. Izyumskaya, M. A. Reshchikov, Ü. Özgür, and H. Morkoç, Phys. Status Solidi (RRL) **4**, 70 (2010).
[32]D. C. Look and R. J. Molnar, Appl. Phys. Lett. **70**, 3377 (1997).
[33]D. C. Look, K. D. Leedy, D. H. Tomich, and B. Bayraktaroglu, Appl. Phys. Lett. **96**, 062102 (2010).
[34]H. Y. Liu, V. Avrutin, N. Izyumskaya, Ü. Özgür, and H. Morkoç, Superlattices Microstruct. **48**, 458 (2010).
[35]H. Y. Liu, V. Avrutin, N. Izyumskaya, Ü. Özgür, A. B. Yankovich, A. V. Kvit, P. M. Voyles, and H. Morkoç, J. Appl. Phys. **111**, 103713 (2012).
[36]Y. Berta, C. Ma, and Z. L. Wang, Micron **33**, 687 (2002).
[37]B. L. Zhu, S. J. Zhu, X. Z. Zhao, F. H. Su, G. H. Li, X. G. Wu, and J. Wu, Phys. Status Solidi A **208**, 843 (2011).